Biosynthesis of Strained Piperazine Alkaloids: Uncovering the Concise Pathway of Herquline A

Xia Yu,[†,§] Fang Liu,[‡] Yi Zou,[†] Man-Cheng Tang,[†] Leibniz Hang,[‡] K. N. Houk,*[,†,‡] and Yi Tang*[,†,‡]

[†]Department of Chemical and Biomolecular Engineering; and [‡]Department of Chemistry and Biochemistry, University of California, Los Angeles, Los Angeles, California 90095, United States

[§]School of Pharmaceutical Sciences, Central South University, Changsha, Hunan 410013, People's Republic of China

Ⓢ Supporting Information

ABSTRACT: Nature synthesizes many strained natural products that have diverse biological activities. Uncovering these biosynthetic pathways may lead to biomimetic strategies for organic synthesis of such compounds. In this work, we elucidated the concise biosynthetic pathway of herquline A, a highly strained and reduced fungal piperazine alkaloid. The pathway builds on a nonribosomal peptide synthetase derived dityrosine piperazine intermediate. Following enzymatic reduction of the P450-cross-linked dicyclohexadienone, N-methylation of the piperazine serves as a trigger that leads to a cascade of stereoselective and nonenzymatic transformations. Computational analysis of key steps in the pathway rationalizes the observed reactivities.

Figure 1. Structures of strained diketopiperazine and piperazine natural products. The X-ray crystal structure of herquline A (1) is from CCDC (id: HERQUL).[10] Also shown is the energy minimized structure of 1.

Building strained molecules is of significant interest to synthetic and physical chemists. The difficulties associated with forging strained connectivities in complex molecules have led to the development of new synthetic strategies.[1] Strained natural products from Nature often possess potent biological activities due to their unique three-dimensional structures. An effective method used by Nature to introduce strain is oxidative cyclization of acyclic precursors.[2] The best-known examples are vancomycin and related glycopeptides, in which three to four aryl rings in a linear heptapeptide precursor are cross-linked to form diphenyl (C–C bond) or diphenyl ether (C–O bond) moieties.[3] Aryl coupling to introduce strain and structural complexity are also observed in other peptides, cyclophanes and plant alkaloids natural products.[4] Therefore, comprehensive understanding of how Nature generates such strained molecules from linear precursors can provide inspiration to development of new synthetic strategies.

One intriguing class of strained peptides consists of those morphed from simple dipeptides, such as mycocyclosin, piperazinomycin and herquline A (1) (Figure 1). Mycocyclosin is a cyclized diketopiperazine produced by *Mycobacterium tuberculosis*.[5,6] The C–C cross-link between the phenol side chains is introduced by a P450 CYP121, using cyclo-Tyr-Tyr as substrate.[6] Structural and computational analysis of CYP121 have shed light on its catalytic mechanism.[6,7] Although the molecular target of mycocyclosin is not known, CYP121 has been found to be essential for virulence of *M. tuberculosis*.[8] Also derived from a dityrosine precursor, the antibiotic piperazinomycin contains a
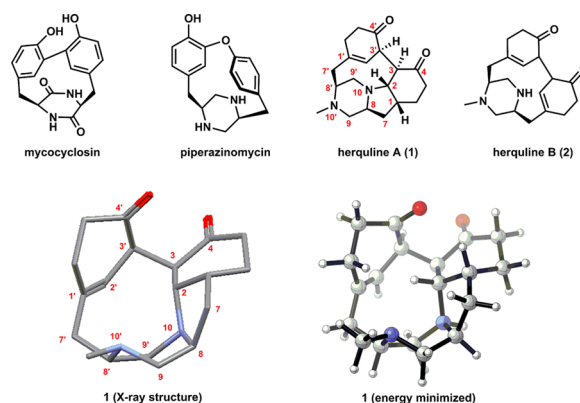
reduced piperazine core and tyrosines cross-linked via a phenyl ether linkage.[9]

Herquline A (1) is a fungal metabolite that inhibits platelet aggregation and replication of the influenza virus.[11] 1 is a pentacyclic (6–9–6–5–6) and strained dipeptide that has undergo significant structural modifications from a presumed dityrosine precursor. In addition to having a reduced piperazine core and a C3–C3′ cross-link between the phenyl side chains, both phenyl rings have undergone further stereoselective reduction to cyclohexanones, thereby injecting chirality at the site of C–C cross-linking. Furthermore, a pyrrolidine moiety fused to the N-methylpiperazine and the cyclohexanone rings is forged through the C2–N10 bond, constraining the conformation of the molecule into a bowl-shaped structure (Figure 1). A related molecule herquline B (2) was isolated from the producing strain, and is a likely biosynthetic intermediate to 1.[12] To date, no synthetic or biosynthetic studies on 1 has been described. Here we report characterization of the biosynthetic pathways to both 1 and 2. We demonstrate this is a highly efficient pathway in which the N10′-methylation step serves as a trigger for forming the multicyclic core of 1.

We first scanned the sequenced genome of the producing strain *Penicillium herquei* for a potential gene cluster of 1.[13] We reasoned that the dipeptide may be derived from a single module NRPS, similar to the reported LnaA enzyme.[14] Of the 10 predicted

NRPS-containing clusters, the six-gene cluster shown in Figure 2A was chosen as the top candidate, because enzymes encoded
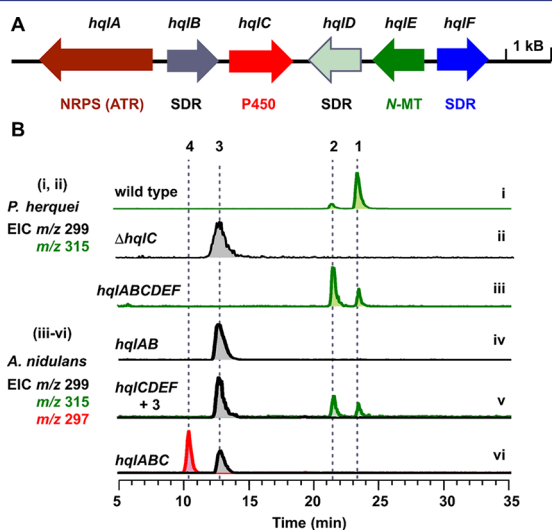

Figure 2. Biosynthesis of the dipeptide **1** by the *hql* gene cluster from *P. herquei*. (A) *hql* gene cluster. Abbreviations: NRPS (nonribosomal peptide synthetase); NRPS domain A, adenylation; T, thiolation; R, reductase. SDR, short-chain dehydrogenase; MT, methyltransferase. (B) Analysis of metabolites from fungal strains. The extracted ion chromatograms (EICs) under positive ionization are shown.

include NRPS (*hqlA*), P450 (*hqlC*) and methyltransferase (*hqlE*). The cluster also encodes three enzymes with homology to short-chain dehydrogenase (SDR) (*hqlB*, *hqlD* and *hqlF*) that may be involved in the extensive reduction en route to **1**. To investigate function of the putative *hql* cluster, we refactored each of the six genes to be under strong *Aspergillus* promoters and introduced them into *A. nidulans* A1145 for heterologous expression (Figure S1). Production of both **1** and **2** were detected and confirmed from the strain (Figure 2B, iii) (for NMR, see Figures S25–S33, Tables S5 and S6).

To investigate the role of the P450 enzyme, a Δ*hqlC* strain of *P. herquei* was constructed (Figure S4). The resulting strain was abolished in the production of **1** and **2**, but instead accumulated a more polar product **3** with *m/z* = 299 (Figure 2B, ii). This compound was isolated and characterized to be the diphenyl piperazine **3** (Scheme 1, for NMR see Figures S34–S38, Table S7),[14] indicating that HqlC is involved in the oxidative coupling of the aryl side chains. Heterologous expression of HqlA and HqlB in

Scheme 1. Functions of HqlA and HqlB

A. nidulans also afforded **3** (Figure 2B, iv). Feeding of **3** to *A. nidulans* expressing the remaining four genes in the pathway (*hqlCDEF*) led to conversion of **1** and **2** (Figure 2B, v), showing **3** is an on-pathway product.

We next investigated the function of the NRPS HqlA and the associated SDR HqlB using purified enzymes from *Escherichia coli* (Figure S5). Incubation of HqlA with L-tyrosine, ATP and NADPH led to the production of predominately **6** (Figure S6), which is a diphenyl pyrazine (Scheme 1). Traces amounts of **5** was also produced but was rapidly oxidized into **6** (Figure S7). Hence, similar to that reported for LnaA,[14] HqlA can activate two molecules of L-tyrosine as tyrosyl-thioesters, reduce them into the corresponding amino aldehydes and form the coupled product **5**. **3** was formed when HqlB was added to the reaction, demonstrating its role in reducing **5** to the piperazine using two equivalents of NADPH.

To probe the function of the P450 HqlC, which shows weak sequence homology to CYP121 from the mycocyclosin pathway (Figure S8),[7] we expressed HqlABC together in *A. nidulans*. A new metabolite **4** was produced (Figure 2B, vi). Purification and characterization of **4** turned out to be challenging. However, on the basis of MS, UV and available NMR signals (Figures S20, S39 and S40), this compound is near certainly the cross-linked diphenyl piperazine (Figure 3). Therefore, HqlC plays the analogous role as CYP121 in forging the strained C−C bond between the phenyl rings, the difference being HqlC uses a piperazine substrate whereas CYP121 acts on a diketopiperazine.[6] A proposed mechanism for HqlC in the oxidative cyclization of **3** into **4** is shown in Figure 3. Although HqlC may employ the same proposed mechanism as CYP121 in generating and coupling two phenyl C-radicals,[7] we propose an alternative single radical addition mechanism. Here abstraction of one phenolic hydrogen yields the radical **10**. The radical can be delocalized to C3 in **11** and can add to the C3′ of the other phenyl ring to give **12**. This can be followed by a second step of hydrogen abstraction and formation of the dicyclohexadienone **13** that can readily aromatize into **4**. A similar coupling mechanism was computationally proposed for the P450 in the griseofulvin pathway.[15]

However, **4** is not an on pathway intermediate to **1**, as feeding of this compound to neither *P. herquei* Δ*hqlC* strain, nor the *A. nidulans* *hqlCDEF* expression strain led to production of the final product **1** (Figure S9). Therefore, we hypothesized that aromatized **4** is a shunt product, whereas the α, β-unsaturated dienone groups in **13** are more likely to be subjected to reduction by the remaining SDR enzymes in the cluster. Because **13** cannot be isolated, we added either *hqlD* or *hqlF* to the *A. nidulans* strain that produced **4** (*hqlABC*). The strain expressing HqlABCF synthesized three new compounds, **7**, **8** and **9**, whereas accumulation of **4** was no longer observed (Figure 4A, i). Compounds **7** and **8** have the same mass (*m/z* = 301) and UV absorbance (Figures S22 and S23), whereas **9** and **3** share the same mass (*m/z* = 299). All three compounds were structurally characterized (Figures S44–S59 and Tables S9–S11).

The structures of **7** and **8** were determined as two isomers of desmethyl-herquline B (Figure 3). Both molecules are symmetrical as indicated by the NMR signals, and the C3−C3′ connectivities are unequivocally confirmed by 2D NMR. The positions of the remaining double bonds in the two cyclohexenone rings were also confirmed, which suggests that HqlF catalyzes the sequential reduction of **13** via **14** as shown in Figure 3. All this evidence suggests that **7** and **8** are stereoisomers differing at the C3 and C3′ positions (3R, 3′R or 3S, 3′S). Interestingly, during purification of **7**, we noticed spontaneous
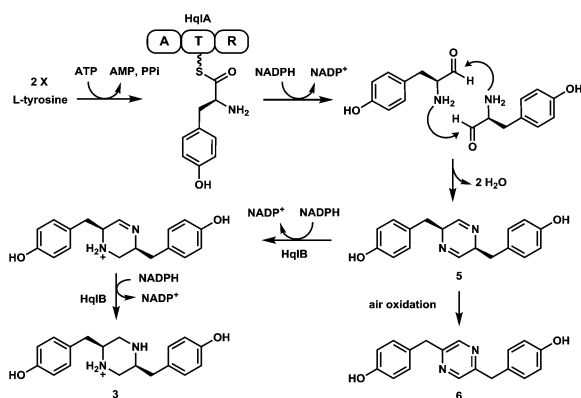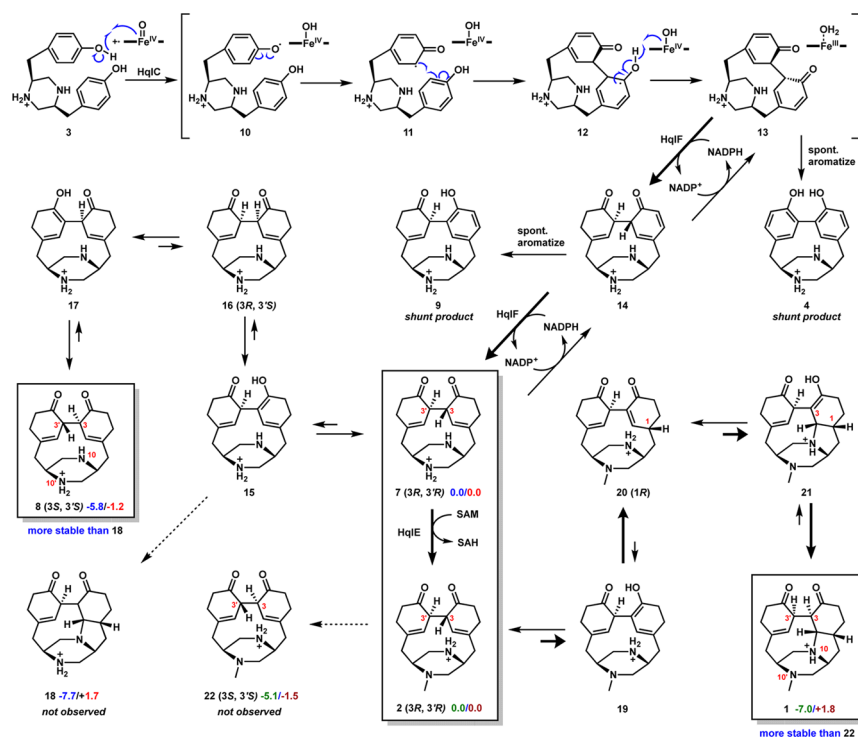
Figure 3. Proposed mechanism for transformation of **3** to **2** and **1**. All piperazine compounds are expected to be protonated at assay conditions. The relative free energies (kcal/mol) of forming **8** and **18** from **7**, as well as those of forming **1** and **22** from **2**, are shown. The blue and green values are calculated using M06-2X/6-31G(d) gas phase basis set, whereas the red and maroon energies used the M06-2X/def2-tzvpp//6-31G(d), SMD in water.

epimerization to **8** (Figure 4B, ii), but not the reverse. This was further shown by feeding studies of these compounds to *A. nidulans* expressing *hqlCDEF* (Figure 4A, ii and iii). When **7** is supplied, both epimerization to **8** and conversion to **1** and **2** were observed; whereas **8** remained unchanged when supplied to the same strain. This stark difference suggests that **7** is an on-pathway stereoisomer, whereas **8** is a more stable shunt product.

To understand the differences in stabilities of the two isomers, we performed DFT calculations on the tautomerization steps that can transform one isomer to the other (Table S13). We propose that inversion of chiral centers from **7** to **8** involves sequential based-catalyzed ketone-enol tautomerization, via the less stable *syn* isomer **16**, as shown in Figure 3. Free energy calculations showed that the *SS* stereoisomer is thermodynamically more stable than the *RR* isomer (by 5.8 and 1.2 kcal/mol in gas and in water, respectively). Comparison of energy minimized structures (Figure S11) of the two isomers showed that the increased stability in *SS* occurs because the CH_2 groups in the piperazine ring point away from the nearby CH_2 groups in the cyclohexenone rings, whereas in the *RR* isomer, the CH_2 groups point into the core of molecule, which leads to a more crowded space between the piperazine and cyclohexenone rings. Furthermore, because the 3′*R* stereochemistry is present at the same position in **1**, we assigned **7** to be in the *RR* configuration, whereas **8** to be the *SS* isomer.

The structure of **9** showed that one of the cyclohexadienone ring was reduced as in **7** and **8**, whereas the other was aromatized to a phenyl ring (Figure 3 and Figures S54−S59). Just as with **4**, **9** is not a substrate of HqlF (Figure S12). This suggests that **9** is a spontaneously aromatized shunt product from **14**, which is the product of one enone reduction by HqlF. To confirm the function of HqlF, we assayed the oxidation of **7** in the presence of NADP⁺. As expected, **9** was indeed observed as a product (Figure 4B, i).

Assay of **8** with HqlF under the same condition did not lead to oxidized products (Figure S12).

The structure of **7** is one *N*-methylation away from the natural product **2**, a reaction that is catalyzed by the methyltransferase HqlE in the gene cluster. Using recombinant HqlE expressed and purified from *E. coli* (Figure S5), we assayed the methylation reaction in the presence of **7** and SAM. The reaction occurred readily as 1 mM of **7** were completely converted to **2** within 2 h in the presence of 1 μM HqlF (Figure 4B, iii). This result, together with NOE data (Figure S13) enabled us to assign the stereochemistry of **2**, which was previously unknown,[12] to be the same 3*R*, 3′*R* as in **7**. Furthermore, we detected spontaneous and slow conversion of **2** to the final product of **1** when placed in Tris buffer at pH 8.0 (Figure 4B, iv). This conversion shows that the stereoselective cyclization of **2** into **1** does not require an enzyme. There is one remaining enzyme in the gene cluster, the SDR HqlD, that is of unassigned function. However, adding HqlD to **2** does not accelerate the conversion to **1**. HqlD was shown to be dispensable in the pathway as excluding it from the refactored pathway in *A. nidulans* has no effect on the final production of **1** and **2** (Figures S3 and S14).

The conversion of **2** to **1** requires tautomerization of one of the cyclohexenone rings in **7** to yield **20**. This is followed by 1,4-Michael addition to form the fused pyrrolidine ring in **21** and ketonization to yield **1**. Three new chiral centers are formed during this conversion in the absence of any enzymatic control. DFT calculations were performed to examine the energetics of these reactions and the likelihood of forming the opposite stereoisomers (Figure S16). The first stereocenter at C1 (1*R*) is formed during tautomerization of **19** to **20**. The 1*S* stereoisomer could be formed if protonation were to take place at the opposite side, but calculations show that the 1*S* isomer is higher in energy than the 1*R* isomer by 2.4 kcal/mol. From the 1*R* configuration in **20**, the second chiral center at C2 in **21** formed by N10 attack on
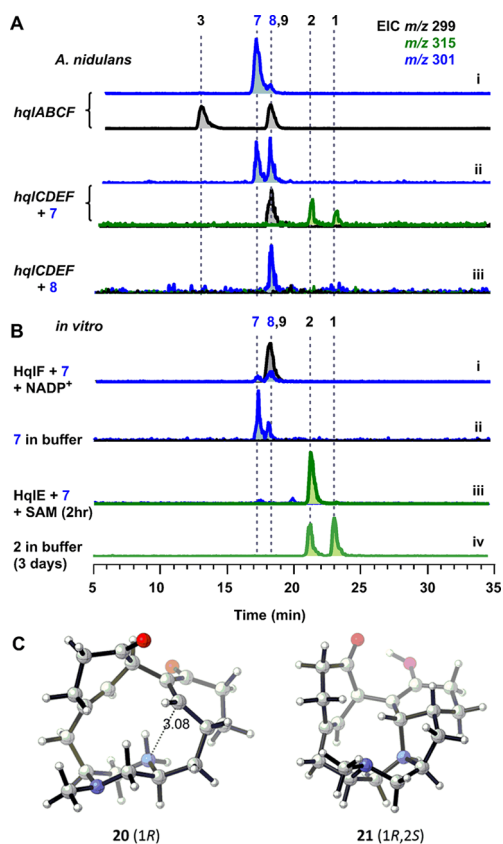
Figure 4. Formation of **1** and **2** requires an SDR HqlF and MT HqlE. (A) Pathway refactoring and chemical complementation in *A. nidulans*. (B) In vitro confirmation of HqlE and HqlF functions, and the spontaneous conversion of **2** to **1**. (C) Computation analysis shows formation of the 2S stereocenter in **21** from **20**.

the β-carbon must be the 2S stereoisomer, as shown in the computed structures in Figure 4C. The third stereocenter at C3 in **1**, formed from the protonation of **21** is the 3R configuration. This is in agreement with computation because the 3S stereoisomer is computed to be 9.3 kcal/mol higher in free energy.

Remarkably, introducing the N10′-methyl group in **2** appears to lock the configuration of the dicyclohexenone system in the 3R,3′R configuration, as the spontaneous tautomerization to the SS product **22** was not observed, in sharp contrast to the conversion of **7** to **8**. On the other hand, spontaneous cyclization of **7** to the herquline like product **18** is also not detected (Figure 3). It is unexpected that a single N10′-methylation step, which breaks symmetry of the molecule, would have such a profound effect on the spontaneous rearrangement steps from **7**. Computations with various functionals, basis sets, and solvation models gave varying energetics (Tables S12−S15), but several trends are revealed by these computations. First, we explored all the intermediates in the conversion of the *RR* isomers (**7** and **2**) to either the *SS* (**8** and **22**) or Michael addition products (**18** and **1**). The energies to form enol intermediates indicate that these transformations should all occur readily at room temperature (Tables S12−S15). Furthermore, the reactions to form either the *SS* isomer, or the Michael addition product are only slightly exergonic, and so both of these reactions are reversible. Consequently, the products formed are controlled by their thermodynamic stabilities rather than their rates of formation. Our calculations have not yet provided a clear indication of why the double epimerization product, **8**, is more stable than the

Michael adduct **18**, yet methylation causes herquline A, **1**, to be more stable than double epimer, **22**.

In summary, in addition to using a P450 to catalyze phenyl coupling, the herquline pathway relies on nonenzymatic steps of which the stereochemical outcomes are strongly influenced by the methylated piperazine core. Such strategies may serve as biomimetic inspiration toward the first total synthesis of herquline A.

■ ASSOCIATED CONTENT

ⓢ Supporting Information

The Supporting Information is available free of charge on the ACS Publications website at DOI: 10.1021/jacs.6b09464.

Experimental details (PDF)

■ AUTHOR INFORMATION

Corresponding Authors

*Y.T. yitang@ucla.edu
*K.N.H. houk@chem.ucla.edu

Notes

The authors declare no competing financial interest.

■ ACKNOWLEDGMENTS

■ REFERENCES

(1) (a) Burns, N. Z.; Krylova, I. N.; Hannoush, R. N.; Baran, P. S. *J. Am. Chem. Soc.* **2009**, *131*, 9172. (b) Baran, P. S.; Burns, N. Z. *J. Am. Chem. Soc.* **2006**, *128*, 3908. (c) Bowie, A. L.; Trauner, D. *J. Org. Chem.* **2009**, *74*, 1581. (d) Beugelmans, R.; Bigot, A.; Bois-Choussy, M.; Zhu, J. *J. Org. Chem.* **1996**, *61*, 771. (e) Cochrane, J. R.; White, J. M.; Wille, U.; Hutton, C. A. *Org. Lett.* **2012**, *14*, 2402.

(2) Sydor, P. K.; Barry, S. M.; Odulate, O. M.; Barona-Gomez, F.; Haynes, S. W.; Corre, C.; Song, L.; Challis, G. L. *Nat. Chem.* **2011**, *3*, 388.

(3) Yim, G.; Thaker, M. N.; Koteva, K.; Wright, G. *J. Antibiot.* **2014**, *67*, 31.

(4) (a) Gulder, T.; Baran, P. S. *Nat. Prod. Rep.* **2012**, *29*, 899. (b) Liu, W. T.; Kersten, R. D.; Yang, Y. L.; Moore, B. S.; Dorrestein, P. C. *J. Am. Chem. Soc.* **2011**, *133*, 18010.

(5) Vetting, M. W.; Hegde, S. S.; Blanchard, J. S. *Nat. Chem. Biol.* **2010**, *6*, 797.

(6) Belin, P.; De, M. H. L.; Fielding, A.; Lequin, O.; Jacquet, M.; Charbonnier, J.-B.; Lecoq, A.; Thai, R.; Courcon, M.; Masson, C.; Dugave, C.; Genet, R.; Pernodet, J.-L.; Gondry, M. *Proc. Natl. Acad. Sci. U. S. A.* **2009**, *106*, 7426.

(7) Dumas, V. G.; Defelipe, L. A.; Petruk, A. A.; Turjanski, A. G.; Marti, M. A. *Proteins: Struct., Funct., Genet.* **2014**, *82*, 1004.

(8) McLean, K. J.; Carroll, P.; Lewis, D. G.; Dunford, A. J.; Seward, H. E.; Neeli, R.; Cheesman, M. R.; Marsollier, L.; Douglas, P.; Smith, W. E.; Rosenkrands, I.; Cole, S. T.; Leys, D.; Parish, T.; Munro, A. W. *J. Biol. Chem.* **2008**, *283*, 33406.

(9) Tamai, S.; Kaneda, M.; Nakamura, S. *J. Antibiot.* **1982**, *35*, 1130.

(10) Furusaki, A.; Matsumoto, T. *J. Chem. Soc., Chem. Commun.* **1980**, 698.

(11) Omura, S.; Hirano, A.; Iwai, Y.; Masuma, R. *J. Antibiot.* **1979**, *32*, 786.

(12) Enomoto, Y.; Shiomi, K.; Hayashi, M.; Masuma, R.; Kawakubo, T.; Tomosawa, K.; Iwai, Y.; Omura, S. *J. Antibiot.* **1996**, *49*, 50.

(13) Gao, S. S.; Duan, A.; Xu, W.; Yu, P.; Hang, L.; Houk, K. N.; Tang, Y. *J. Am. Chem. Soc.* **2016**, *138*, 4249.

(14) Forseth, R. R.; Amaike, S.; Schwenk, D.; Affeldt, K. J.; Hoffmeister, D.; Schroeder, F. C.; Keller, N. P. *Angew. Chem., Int. Ed.* **2013**, *52*, 1590.

(15) Grandner, J. M.; Cacho, R. A.; Tang, Y.; Houk, K. N. *ACS Catal.* **2016**, *6*, 4506.